Bioorganic & Medicinal Chemistry 23 (2015) 6807–6814

Contents lists available at ScienceDirect

Bioorganic & Medicinal Chemistry

journal homepage: www.elsevier.com/locate/bmc

Isomeric methoxy analogs of nimesulide for development of brain cyclooxygense-2 (COX-2)-targeted imaging agents: Synthesis, in vitro COX-2-inhibitory potency, and cellular transport properties

Yumi Yamamoto [a,*], Takuya Hisa [a], Jun Arai [a], Yohei Saito [a], Fumihiko Yamamoto [a], Takahiro Mukai [b], Takashi Ohshima [c], Minoru Maeda [d], Yasuhito Ohkubo [a]

[a] Tohoku Pharmaceutical University, 4-4-1, Komatsushima, Aoba-ku, Sendai, Miyagi 981-8558, Japan
[b] Kobe Pharmaceutical University, 4-19-1 Motoyama Kitamachi, Higashinada-ku, Kobe 658-8558, Japan
[c] Graduate School of Pharmaceutical Sciences, Kyushu University, 3-1-1 Maidashi, Higashi-ku, Fukuoka 812-8582, Japan
[d] Daiichi University of Pharmacy, 22-1 Tamagawa-cho, Minami-ku, Fukuoka 815-8511, Japan

ARTICLE INFO

Article history:
Received 27 July 2015
Revised 3 October 2015
Accepted 5 October 2015
Available online 8 October 2015

Keywords:
Nimesulide
Methoxy substituted analog
COX-2
Caco-2 cells

ABSTRACT

Nimesulide analogs bearing a methoxy substituent either at the *ortho*-, *meta*- or *para*-position on the phenyl ring, were designed, synthesized, and evaluated for potential as radioligands for brain cyclooxygenase-2 (COX-2) imaging. The synthesis of nimesulide and regioisomeric methoxy analogs was based on the copper-mediated arylation of phenolic derivatives for the construction of diaryl ethers. These isomeric methoxy analogs displayed lipophilicity similar to that of nimesulide itself, as evidenced by their HPLC log$P_{7.4}$ values. In vitro inhibition studies using a colorimetric COX (ovine) inhibitor-screening assay demonstrated that the *para*-methoxy substituted analog retains the inhibition ability and selectivity observed for parent nimesulide toward COX-2 enzyme, whereas the *meta*- and *ortho*-methoxy substituents detrimentally affected COX-2-inhibition activity, which was further supported by molecular docking studies. Bidirectional transport cellular studies using Caco-2 cell culture model in the presence of the P-glycoprotein (P-gp) inhibitor, verapamil, showed that P-gp did not have a significant effect on the efflux of the *para*-methoxy substituted analog. Further investigations using the radiolabeled form of the *para*-methoxy substituted analog is warranted for in vivo characterization.

1. Introduction

Cyclooxygenase (COX) is a critical enzyme that catalyzes the biosynthesis of prostaglandin from arachidonic acid. It has at least two isoforms (COX-1 and COX-2). COX-2 enzyme is expressed in response to inflammatory stimuli. While COX-2 is not expressed in most tissues, high levels of COX-2 were reported in lung, colon, and breast cancer.[1–3] The brain is one of the organs that constitutively expresses COX-2. COX-2 was reported to play a role in physiological control of synaptic plasticity and neurological disorders including cerebrovascular and neurodegenerative disorders such as Alzheimer's and Parkinson's diseases.[4,5] While COX-2 was reported to regulate physiologic functions, role of COX-2 in pathogenic mechanisms is largely unclear.[6] To investigate the expression and activity of COX-2 in related disorders in vivo, considerable interest was focused on nuclear imaging technology such as positron emission tomography (PET) or single photon emission computed tomography (SPECT), both for diagnostic and research purposes.[7] As reviewed by Laube et al.,[8] arachidonic acid (substrate of COX) was labeled with ^{11}C by Channing et al. in 1993.[9] In 2002, McCarthy et al. reported synthesis and in vitro/in vivo evaluations of the ^{18}F labeled COX-2 inhibitor, SC58125.[10] Since then, traditional anti-inflammatory drugs (classical NSAIDS) and selective COX-2 therapeutic agents were considered as candidate radioligands for detecting COX-2 expression in vivo by using PET and/or SPECT, and their potential was extensively investigated. In 2005, Toyokuni et al. performed a PET study in vervet monkeys,[11] and in 2006, Tanaka et al. evaluated in vitro transcellular transport in human cells.[12] In these ways, radioligand candidates for COX-2 imaging were evaluated from various perspectives in the late 2000s. Prabhakaran et al. performed PET studies in Sprague–Dawley rats and in a baboon in 2007.[13] They reported penetration of the blood–brain barrier and the lower de-^{18}F-fluorination rates in baboons compared to rodents; however, their radioligand candidate showed fast metabolism. As reported in their study and in

* Corresponding author. Tel.: +81 22 727 0121; fax: +81 22 727 0165.
E-mail address: yumi-y@tohoku-pharm.ac.jp (Y. Yamamoto).

http://dx.doi.org/10.1016/j.bmc.2015.10.007
0968-0896/

another recent review,[8,14] radioligand candidates do not have significant in vivo application owing to commonly reported problems including poor brain penetration, non-specific uptake in the brain, and rapid radioligand metabolism. However, despite these shortcomings, some beneficial role of COX-1 and/or COX-2 was revealed gradually. For example, studies about microglia using ^{11}C-PK11195 suggested that COX-1 and/or COX-2 play a role in neuroinflammation.[15,16] There are no satisfactory PET and SPECT ligands for imaging COX-2 even now; however, several radiolabeled COX-2 inhibitors are being synthesized, evaluated, and reported constantly. In 2015, Kaur et al. synthesized and evaluated ^{18}F-celecoxib derivatives.[17]

N-(4-Nitro-2-phenoxyphenyl)methanesulfonamide (nimesulide) is a well-known COX inhibitor with increased selectivity for COX-2. It exhibits potent analgesic and antipyretic properties with an effect on aromatase suppression; however, it might lead to significant hepatic damage.[18–20] Nimesulide was reported to possess brain penetration activity, as evidenced from pharmacokinetic and tissue distribution studies after systemic administration in animals.[21–24] In addition, the reported log*P* value lies in the lipophilicity range of brain-targeted nuclear imaging agents. Moreover, in an in vitro study with Caco-2 cells, reported nimesulide as a non-substrate for brain efflux transporter, P-glycoprotein (P-gp) (also called as ABCB1), which restricts the uptake of intravenously injected radioligands in the brain.[25] The structural analysis of nimesulide-based analogs revealed the importance of the nitro group and methanesulfonamide group for COX-inhibition activity and selectivity.[26,27] Based on the pharmacological and physiochemical characteristics, we believed that modification of nimesulide would yield an effective radioligand for imaging brain COX-2 with PET or SPECT. Thus, as a next step of our research on COX-targeted radiopharmaceuticals,[28] we became involved in the development of nimesulide analogs with a methoxy substituent as a potential labeling site with the positron-emitter carbon-11 ($T_{1/2}$ = 20.4 min), attached to the phenyl ring of the molecule (Fig. 1). The insertion of a hydrophilic methoxy group into molecules with COX-2-inhibitory activity was often regarded as one of the molecular modification strategies to alter the pharmacological properties of a molecule.[29] This article describes the synthesis and lipophilicity of methoxy-substituted analogs of nimesulide. The COX-1/COX-2-inhibitory activities in an in vitro assay and their interaction with P-gp in Caco-2 cell line are characterized in this study.

2. Results and discussion

2.1. Synthesis of nimesulide and methoxy-substituted analogs

The synthesis of nimesulide by nitration of *N*-(2-phenoxyphenyl)-methanesulfonamide was described in the US patent literature.[30] With a view to develop a radiolabeled molecule, our synthetic approach was developed to obtain the target compounds, nimesulide **1a** and its analogs **1b–d**, bearing a single methoxy substituent at either *ortho*-, *meta*- or *para*-position of the phenyl ring, based on the copper-mediated arylation of phenols, as outlined in Scheme 1. The synthesis was initiated with 2-amino-5-nitrophenol, which was converted into the *N*-phthalimide derivative **2** by reaction with phthalic anhydride according to the described procedure, to protect the amino group.[31] $Cu(OAc)_2$-catalyzed coupling of **2** with aryl boronic acid in the presence of pyridine as base and pyridine *N*-oxide as oxidant yielded satisfactory yields of diaryl ethers **3a–d**.[32,33] The use of pyridine *N*-oxide as an additive led to more facile coupling. The coupling reaction with *ortho*-methoxyphenyl boronic acid was difficult owing to steric effect. The subsequent de-protection by reduction with hydrazine monohydrate resulted in the 4-nitroaniline derivatives **4a–d** with a quantitative yield. Finally, treatment of **4a–d** with excess methanesulfonyl chloride in triethylamine–CH_2Cl_2, followed by refluxing in 3 M NaOH, led to the requisite compounds **1a–d** at 66–73% yields. The structures of all compounds were characterized by ^{1}H NMR and high-resolution mass spectrometry.

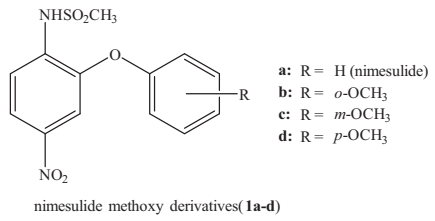

Figure 1. Representation of chemical structures of compounds (**1a–d**).

2.2. Lipophilicity

Lipophilicity is an important factor that influences passive brain entry of intravenously administered compounds. It was reported that compounds with log$P_{7.4}$ values (logarithm of the *n*-octanol/water partition coefficient, at pH 7.4) in the range of 2.0–3.5 exhibit optimal passive brain entry in vivo.[34] Nimesulide molecule **1a** with a weak acidic sulfonamide group has a pK_a value of 6.4–6.8;[18,35,36] therefore its lipophilicity is pH-dependent. Previous studies reported that nimesulide **1a** exhibited lipophilicity with a log$P_{7.4}$ value of 1.48 in octanol/water system[36] and log$D_{7.4}$ value of 1.58 as analyzed by HPLC C_{18} methodology.[36] In this study, we estimated the partition coefficients (log$P_{7.4}$) of compounds **1a–d** at pH 7.4 according to the OECD guidelines for testing of chemicals 117, using reversed-phase HPLC method[37] owing to its high reproducibility and resistance to impurities present in the samples. The results are shown in Table 1, including the log$P_{7.4}$ value of the reference, nimesulide for comparison. The estimated log$P_{7.4}$ values of three methoxy regioisomers are quite similar (log$P_{7.4}$ = 1.26–1.65) and comparable to that for nimesulide itself (log$P_{7.4}$ = 1.61), thus supporting their relatively low hydrophobicity.

In this study, only the partition coefficient of the compounds at pH 7.4 were considered according to the previously reported log*P* values of the neutral and anion forms of nimesulide by Tsantili-Kakoulidou et al., the neutral form was calculated to be only 480-fold as lipophilic as its anion form.[37] A similar log*D*/pH profile could be expected in the case of its methoxy substituted analogs. Mazak et al. recently demonstrated dominance of the ionic species in the lipophilicity profile.[38,39] Thus, it is conceivable that the contribution of the charged species to the overall lipophilicity for the isomeric methoxy analogs might be crucial for the biological lipophilicity-related processes.

2.3. In vitro COX-inhibitory potency

The selectivity and affinity toward COX-2 were considered as the initial criteria for a prospective imaging agent. Compounds **1a–d** are derivatives of nimesulide and expected to bind at the COX-2 active site. COX-2 inhibitory potency may correlate with COX-2 binding affinity if the compounds bind at the active site. The inhibitory potency of the compounds (**1a–d**) for the COX enzyme and selectivity was determined in vitro by using a colorimetric COX (ovine) inhibitor-screening assay (pH = 8.0). The activity of reference compounds celecoxib and indomethacin was also included. The IC_{50} value was calculated from the concentration–inhibition response curve.

As shown in Table 2, the *para*-methoxy isomeric analog **1d** displayed moderate inhibitory activity against COX-2 with an

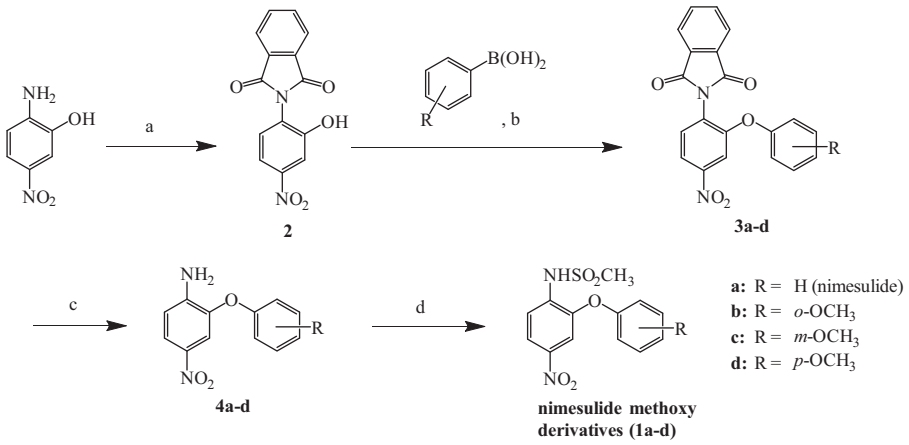

Scheme 1. Reagents and conditions: (a) phthalic anhydride, AcOH, reflux, 6 h; (b) $Cu(OAc)_2$, dry pyridine, MS 4 Å, dry CH_2Cl_2, O_2, rt, 72 h; (c) hydrazine monohydrate, MeOH, reflux, 6 h; (d) (1) CH_3SO_2Cl, dry Et_3N, dry CH_2Cl_2, rt, 23 h, (2) 3 M NaOHaq, 90 °C, 16 h.

Table 1
Lipophilicity of compounds **1a–d** measured by using HPLC method

Compounds	log $P_{7.4}$
Nimesulide (**1a**)	1.61 ± 0.02
o-OCH_3 (**1b**)	1.26 ± 0.01
m-OCH_3 (**1c**)	1.65 ± 0.01
p-OCH_3 (**1d**)	1.41 ± 0.00

Average ± SD (n = 3).

IC_{50} value of 2.31 μM and a selectivity index of 43 for COX-2, indicating equipotency to the parent nimesulide. However, the *para*-isomer **1d** displayed both reduced inhibitory activity and selectivity for COX-2 compared with the known COX-2 inhibitor, celecoxib. In contrast to the inhibitory activity of the *para*-methoxy isomer **1d**, interestingly, the great loss of inhibitory activity toward COX-2 was displayed by *ortho*- and *meta*-methoxy isomers **1b** and **1c**. Thus, the position of the methoxy substituent on the phenyl ring is crucial for COX-2-inhibition activity. Meanwhile, none of the tested compounds showed inhibitory activity on COX-1 enzyme down to IC_{50} values of 100 μM.

In order to further understand the structure–activity relationship of compounds **1a–d** at COX-2 active site, we performed the docking simulations using Discovery Studio 4.0 software program. The molecular docking studies were performed using the CDOCKER protocol, the receptor–ligand interaction protocol that employs the CHARMm force field.[40] The results of the docking procedure with two poses of compounds **1a** and **1d** are shown in Figure 2.

According to the docking studies of nimesulide and COX-2 active site in the literature, there are two docking poses; 'lateral mode' and 'inverse mode'.[41–43] In the "lateral mode" (also called as 'orientation A' or 'pose P1'), the nitro group of nimesulide was located close to Arg120 and Ile345, and the methanesulfonamide group was located close to Phe518, Arg513, and His90. On the other side, in the 'inverse mode' (also called as 'orientation B' or 'pose P9'), the nitro group of nimesulide was located close to the Phe518, Arg513 and His90, and the methanesulfonamide group was located close to the Arg120 and Ile345. Garcia-Nieto et al. analyzed the molecular dynamic simulations and reported that both binding poses equally contributed to COX-2-inhibitory activity of nimesulide, with similar interaction energies.[43] In addition, our docking simulations of nimesulide (**1a**) and COX-2 yielded two poses, which was in agreement with these studies.

Considering the docking poses of compounds (**1b–d**), **1d** displays two poses similar to that of nimesulide, especially the active orientation of the COX-2 pharmacophore (NO_2, SO_2NH) on the nitrophenyl ring (Fig. 2), although **1b** and **1c** were not positioned to accommodate the pharmacophore. According to our calculation, appropriate free binding energies predicting abundance ratio of each poses and COX-2-inhibitory potency were not analyzed because of rigid structure of protein. However, **1b** and **1c** did not show even local minima with favorable pose. A molecular modeling study of nimesulide by Pattabhi et al. suggested that the phenyl ring is present in a hydrophobic cavity comprising several amino acid residues within the COX-2 binding site.[27] This hydrophobic pocket appears large enough to accommodate the methoxy-substituted phenoxy fragment of the molecule. Moreover, Julemont et al. have proposed, based on the structure–activity studies, that for nimesulide, the inhibition of COX enzymes requires anionic sulfonanimde species.[26] A possible explanation for the observed positional influences of the methoxy substituent could be that the *ortho*- and *meta*-methoxy moiety could distort the active orientation of the COX-2 pharmacophore (NO_2, SO_2NH) on the nitrophenyl ring, thereby reducing the COX-2-inhibitory activity. Further studies are required to understand the interaction mechanism between these compounds and COX-2 enzyme.

Table 2
COX inhibitory potency of four compounds (**1a–d**) and two reference drugs

Compounds	IC_{50}[a] (μM)		Selectivity[b]
	COX-1	COX-2	
Nimesulide (**1a**)	>100	1.92	>52
o-OCH_3 (**1b**)	>100	>100	—
m-OCH_3 (**1c**)	>100	>100	—
p-OCH_3 (**1d**)	>100	2.31	>43
Indomethacin	0.79	11.8	0.067
Celecoxib	>100	0.56	>178

[a] Data derived from colorimetric inhibition screening assay, average of independent 2 assays.
[b] Ratio of $IC_{50(COX\text{-}1)}/IC_{50(COX\text{-}2)}$.

2.4. In vitro transport studies in Caco-2 cells

It is well established that the blood–brain barrier (BBB) contains efflux pumps including the P-gp, which acts as a main barrier for brain-targeted radioligands for in vivo imaging as well as pharmaceutical agents.[44,45] In this study, the cellular transport of nimesulide **1a** and its regioisomeric methoxy analogs **1b**,**c**,**d** were evaluated in a Caco-2 cell culture model at pH 7.2 and 37 °C. Caco-2 cells, the most widely used model for estimation of drug

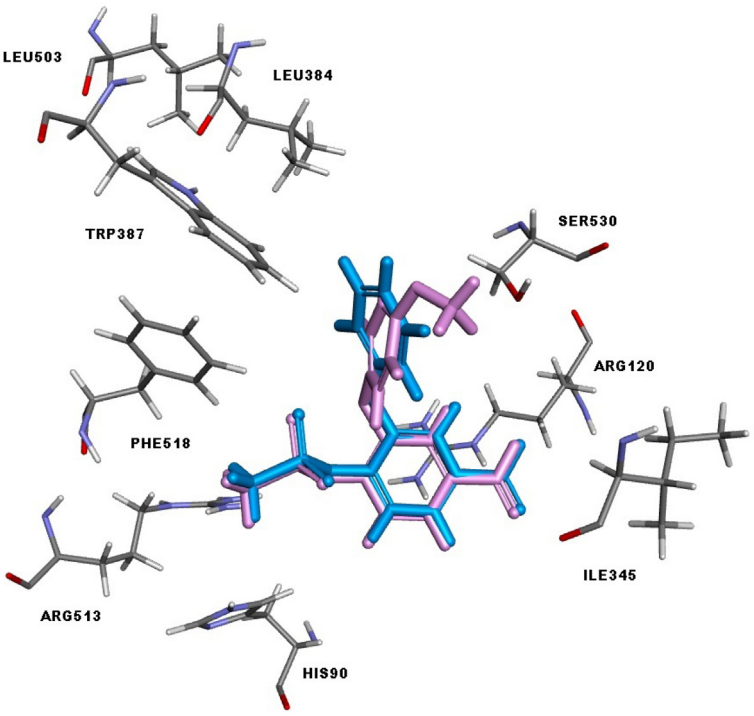

A- lateral mode

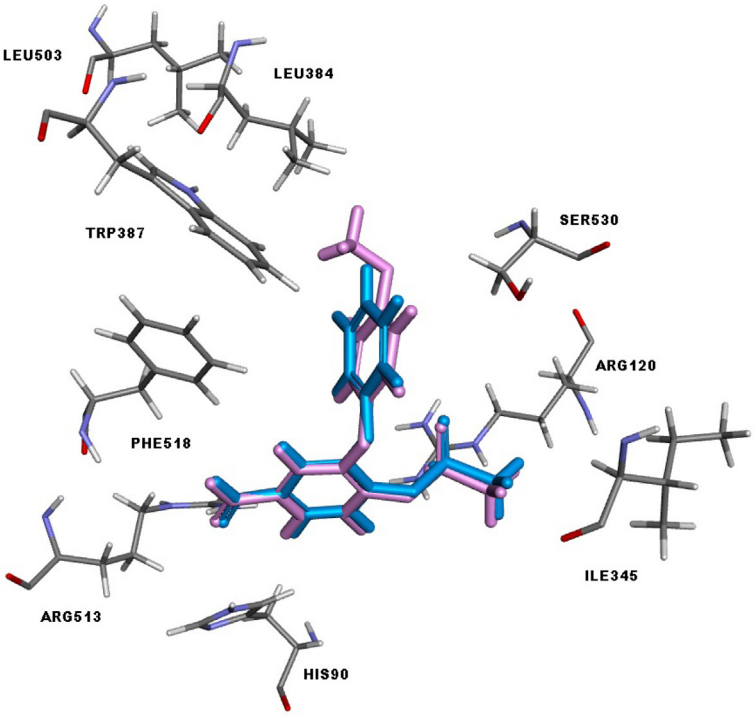

B- inverse mode

Figure 2. Depiction of 'lateral mode' and 'inverse mode' of nimesulide (**1a**, blue) and **1d** (pink) docked at COX-2 active site.

intestine permeability, are often utilized as an in vitro alternative approach for studying drug efflux characteristics. However, there are some limitations to the use of Caco-2 cells as in vivo BBB models.[46–50] In the Caco-2 cells used in this study, a 3.4-fold increase in mRNA expression of P-gp was confirmed at the end of the culture period (data not shown).

Apparent bidirectional permeability ($P_{app,\ A\rightarrow B}$ and $P_{app,\ B\rightarrow A}$) as well as efflux ratio ($P_{app,\ B\rightarrow A}/P_{app,\ A\rightarrow B}$) were initially determined for all the compounds (**1a**–**d**) with two different concentrations (1 μM and 10 μM) in the absence of P-gp inhibitor. In general, compounds displaying efflux ratio below or close to 1 were considered to be transported by passive diffusion or undergo an effective

influx, whereas high ratios (double) were considered as indicative of compounds undergoing effective efflux.[51,52] In this study, slightly higher permeation coefficients in the apical-to-basolateral direction ($P_{app,\ A\rightarrow B} > P_{app,\ B\rightarrow A}$), than those in the reverse direction were observed for all test compounds, thus resulting in the efflux ratios values of <1.0.

The *para*-methoxy isomer **1d** and nimesulide **1a** exhibiting COX-2-inhibitory potency and selectivity, were chosen for further transport studies using the same cells in the presence of the P-gp inhibitor, verapamil at a higher concentration (500 μM). Concurrently, the functionality of P-gp expressed in the Caco-2 cells was determined by using P-gp substrate rhodamine123 as a positive control. Rhodamine123 displayed an efflux ratio of 17.16 under normal conditions, which decreased significantly to 0.71 in the presence of verapamil (500 μM). This indicates the presence of active P-gp in Caco-2 cells and the ability of verapamil to modulate the P-gp-mediated efflux transport. As shown in Table 4, compared to control, the addition of verapamil did not induce significant effect on the efflux ratios for each compound (**1d**,**1a**), suggesting that P-gp-mediated efflux was not involved in the transport of **1d** and **1a** across the Caco-2 cells. This feature might be beneficial for the development of a brain COX-2-targeted radioligand. Our in vitro results for nimesulide **1a** are in agreement with those reported in a previous study by Zrieki et al.[25] The study reported that the exposure of Caco-2 cells to COX inhibitors including nimesulide, although with long-term treatment (14 days), led to down-regulation of P-gp. This could indicate the existence of an interaction or binding sites on P-gp for these COX inhibitors.

The Caco-2 cell lines express other transporters,[53,54] which potentially contribute to the Caco-2 permeability for the compounds used in this study. The organic anion transporter system carrying organic anion species to brain is one of the transporters functionally expressed at the BBB at much lower levels than P-gp.[55] It was found that lumiracoxib, a weakly acidic COX-2 inhibitor, exhibited an inhibitory effect on organic anion transporters (hOAT1 and hOAT3).[56] A similar interaction might be responsible for permeability of nimesulide-related compounds owing to their negative charge.

3. Conclusions

We designed and synthesized three isomeric methoxy-substituted analogs of nimesulide for the development of brain COX-2-imaging radiotracer. Only *para*-methoxy analog **1d** displayed a moderate inhibitory potency and selectivity for COX-2 enzyme, equipotent to the parent nimesulide, whereas the other two analogs **1b** and **1c** displayed robust decrease in COX-2-inhibitory activity. Transport studies using Caco-2 cells showed that P-gp was not involved in the cellular transport of *para*-methoxy isomer **1d** and nimesulide **1a**. However, a poor correlation between conventional in vitro Caco-2 permeability and in vivo brain penetration of radiotracers was recently described in the literature;[57] further studies are warranted to clarify the in vivo characteristics of *para*-methoxy analog **1d** in the radiolabeled form.

4. Experimental

4.1. Synthesis

All chemicals, reagents, and solvents were of the highest purity available and used without further purification. The progress of the reactions was monitored by TLC on Silica Gel 60 F_{254} glass plates (Merck Millipore, Darmstadt, Germany) and spots were visualized under UV light. Column chromatography was performed with Silica gel 60 Å, 200–400 mesh (Sigma–Aldrich Inc., St. Louis, MO, USA). All melting points were determined on a Yanaco melting point apparatus (Yanagimoto Ind. Co., Kyoto, Japan) and are uncorrected. ^{1}H NMR spectra were recorded on JNM-LA600 (JEOL Ltd, Tokyo, Japan) NMR spectrometer using TMS as an internal standard in DMSO-d_6 and the chemical shifts are reported in δ (ppm). IR spectra were recorded with Spectrum One FT-IR Spectrometer (PerkinElmer, Inc., Waltham, MA, USA). EI-MS and High-resolution EI-MS spectra were recorded on JMS-700 (JEOL Ltd, Tokyo, Japan).

4.1.1. Synthesis of 2-(2-hydroxy-4-nitrophenyl)isoindoline-1,3-dione (2)

A solution of 2-amino-5-nitrophenol (3000 mg, 19.5 mmol) and phthalic anhydride (2880 mg, 19.5 mmol) in glacial acetic acid (30 mL) was heated under reflux for 4 h. After cooling, distilled water was added to the reaction mixture and filtered by suction filtration. The solid residue was recrystallized from EtOH to provide **2** (4989 mg, 90.2%) as a beige powder: mp: 322–324 °C; ^{1}H NMR (600 MHz, DMSO-d_6) δ ppm: 10.97 (s, 1H), 7.99 (dd, J = 3.1, 5.5 Hz, 2H), 7.92 (dd, J = 3.1, 5.2 Hz, 2H), 7.81 (dd, J = 2.4, 8.3 Hz, 1H), 7.78 (d, J = 2.4 Hz, 1H), 7.61 (d, J = 8.3 Hz, 1H); FTIR(KBr) cm^{-1}: 3379, 1713; EI-MS m/z: 284 [M]$^+$; HR-MS: Calcd for $C_{14}H_8N_2O_5$ [M]$^+$: 284.0433. Found 284.0432.

4.1.2. Synthesis of 2-(4-nitro-2-phenoxyphenyl)isoindoline-1,3-dione (3a)

To a reaction mixture containing **2** (1000 mg, 3.5 mmol), phenyl boronic acid (1287 mg, 10.6 mmol), Copper(II) acetate (1278 mg 7.0 mmol) and molecular sieves 4 Å (6.0 g) was added anhydrous CH_2Cl_2 (35.2 mL) containing pyridine *N*-oxide (368 mg, 3.9 mmol). After further addition of dry pyridine (1.4 mL, 17.6 mmol), the resulting mixture was allowed to stir at room temperature in an atmosphere of O_2 for 72 h. The reaction was then quenched with distilled water and filtered by suction filtration. The filtrate was washed with 10% HCl, dried and filtered, and the solvent was removed in vacuo. The residue was purified by chromatography on silica gel with $CHCl_3$/hexane/acetone = 2:21:2 to provide **3a** (778.4 mg, 61.4%) as a pale brown powder: mp: 149–150 °C; ^{1}H NMR (600 MHz, DMSO-d_6) δ ppm: 8.16 (dd, J = 2.6, 8.6 Hz, 1H), 7.98 (dd, J = 2.9, 5.6 Hz, 2H), 7.91 (dd, J = 3.1, 5.5 Hz, 2H), 7.88 (d, J = 8.8 Hz, 1H), 7.69 (d, J = 2.4 Hz, 1H), 7.39 (t, J = 8.0 Hz, 2H), 7.20 (t, J = 7.4 Hz, 1H), 7.07 (d, J = 8.0 Hz, 2H); FTIR(KBr) cm^{-1}: 1736, 1716, 1589; EI-MS m/z: 360 [M]$^+$; HR-MS: Calcd for $C_{20}H_{12}N_2O_5$ [M]$^+$: 360.0746. Found 360.0748.

4.1.3. Synthesis of 2-(2-(2-methoxyphenoxy)-4-nitrophenyl) isoindoline-1,3-dione (3b)

Compound **3b** was obtained in a similar manner to the synthesis of **3a** from **2** using 2-methoxy phenyl boronic acid. The crude product was purified by chromatography on silica gel with $CHCl_3$/hexane/acetone = 1:8:1 to provide **3b** (55.7 mg, 40.6%) as a pale brown powder: mp: 198–199 °C; ^{1}H NMR (600 MHz, DMSO-d_6) δ ppm: 8.10 (dd, J = 2.6, 8.8 Hz, 1H), 8.02 (dd, J = 2.9, 5.5 Hz, 2H), 7.95 (dd, J = 2.9, 5.5 Hz, 2H), 7.85 (d, J = 8.4 Hz, 1H), 7.45 (d, J = 2.7 Hz, 1H), 7.26 (t, J = 7.9 Hz, 1H), 7.16 (d, J = 8.2 Hz, 1H), 7.14 (d, J = 8.1 Hz, 1H), 7.00 (t, J = 7.7 Hz, 1H), 3.67 (s, 3H); FTIR(KBr) cm^{-1}: 1715, 1527, 1499; EI-MS m/z: 390 [M]$^+$; HR-MS: Calcd for $C_{21}H_{14}N_2O_6$ [M]$^+$: 390.0852. Found 390.0853.

4.1.4. Synthesis of 2-(2-(3-methoxyphenoxy)-4-nitrophenyl) isoindoline-1,3-dione (3c)

Compound **3c** was obtained in a similar manner to the synthesis of **3a** from **2** using 3-methoxy phenyl boronic acid. The crude product was purified by chromatography on silica gel with $CHCl_3$/hexane/acetone = 1:8:1 to provide **3c** (89.5 mg, 65.2%) as a pale yellow powder: mp: 172–173 °C; ^{1}H NMR (600 MHz, DMSO-d_6) δ

ppm: 8.18 (dd, J = 2.4, 8.6 Hz, 1H), 7.99 (dd, J = 3.1, 5.3 Hz, 2H), 7.93 (dd, J = 2.9, 5.5 Hz, 2H), 7.88 (d, J = 8.8 Hz, 1H), 7.76 (d, J = 2.6 Hz, 1H), 7.28 (t, J = 7.7 Hz, 1H), 6.76 (m, 1H), 6.62 (m, 2H), 3.69 (s, 3H); FTIR(KBr) cm^{-1}: 1736, 1716, 1605; EI-MS m/z: 390 $[M]^+$; HR-MS: Calcd for $C_{21}H_{14}N_2O_6$ $[M]^+$: 390.0852. Found 390.0853.

4.1.5. Synthesis of 2-(2-(4-methoxyphenoxy)-4-nitrophenyl) isoindoline-1,3-dione (3d)

Compound **3d** was obtained in a similar manner to the synthesis of **3a** from **2** using 4-methoxy phenyl boronic acid. The crude product was purified by chromatography on silica gel with $CHCl_3$/hexane/acetone = 1:8:1 to provide **3d** (87.5 mg, 63.7%) as a pale yellow solid: mp: 62–64 °C; ^1H NMR (600 MHz, DMSO-d_6) δ ppm: 8.12 (dd, J = 2.4, 8.6 Hz, 1H), 8.02 (dd, J = 3.1, 5.7 Hz, 2H), 7.95 (dd, J = 2.9, 5.5 Hz, 2H), 7.86 (d, J = 8.8 Hz, 1H), 7.57 (d, J = 2.6 Hz, 1H), 7.08 (d, J = 6.8 Hz, 2H), 6.99 (d, J = 6.8 Hz, 2H), 3.75 (s, 3H); FTIR(KBr) cm^{-1}: 1738, 1534, 1505; EI-MS m/z: 390 $[M]^+$; HR-MS: Calcd for $C_{21}H_{14}N_2O_6$ $[M]^+$: 390.0852. Found 390.0853.

4.1.6. Synthesis of 4-nitro-2-phenoxyaniline (4a)

A solution of **3a** (500 mg, 1.4 mmol) in MeOH (13.9 mL) was treated with hydrazine monohydride (344 μL, 7.1 mmol). Afterwards, the mixture was heated under reflux for 6 h. The resulting mixture was concentrated in vacuo. The residue was diluted with 10% NaOHaq and extracted with $CHCl_3$. The combined organic phases were dried and filtered, and the solvent was removed in vacuo. The residue was purified by chromatography on silica gel with $CHCl_3$/hexane/acetone = 1:8:1 to provide **4a** (310.2 mg, 97.0%) as a yellow solid: mp: 111–112 °C; ^1H NMR (600 MHz, DMSO-d_6) δ ppm: 7.85 (dd, J = 2.2, 9.8 Hz, 1H), 7.45 (d, J = 2.4 Hz, 1H), 7.41 (t, J = 7.8 Hz, 2H), 7.17 (t, J = 7.2 Hz, 1H), 7.06 (d, J = 8.0 Hz, 2H), 6.83 (d, J = 8.4 Hz, 1H), 6.64 (s, 2H); FTIR(KBr) cm^{-1}: 3476, 3352, 1624; EI-MS m/z: 230 $[M]^+$; HR-MS: Calcd for $C_{12}H_{10}N_2O_3$ $[M]^+$: 230.0691. Found 230.0687.

4.1.7. Synthesis of 2-(2-methoxyphenoxy)-4-nitroaniline (4b)

Compound **4b** was obtained in a similar manner to the synthesis of **4a** from **3b**. The product was obtained without purification (26.5 mg, 99.4%) as a yellow solid: mp: 133–134 °C; ^1H NMR (600 MHz, DMSO-d_6) δ ppm: 7.78 (dd, J = 2.6, 9.2 Hz, 1H), 7.28 (dt, J = 1.5, 7.7 Hz, 1H), 7.23 (dd, J = 1.6, 8.2 Hz, 1H), 7.13 (dd, J = 1.6, 7.9 Hz, 1H), 7.09 (d, J = 2.6 Hz, 1H), 7.03 (dt, J = 1.6, 7.6 Hz, 1H), 6.78 (d, J = 8.8 Hz, 1H), 6.70 (s, 2H), 3.77 (s, 3H); FTIR(KBr) cm^{-1}: 3473, 3352, 1624; EI-MS m/z: 260 $[M]^+$; HR-MS: Calcd for $C_{13}H_{12}N_2O_4$ $[M]^+$: 260.0797. Found 260.0791.

4.1.8. Synthesis of 2-(3-methoxyphenoxy)-4-nitroaniline (4c)

Compound **4c** was obtained in a similar manner to the synthesis of **4a** from **3c**. The product was obtained without purification (33.3 mg, 99.9%) as a yellow solid: mp: 122–123 °C; ^1H NMR (600 MHz, DMSO-d_6) δ ppm: 7.87 (dd, J = 2.6, 9.2 Hz, 1H), 7.49 (d, J = 2.6 Hz, 1H), 7.31 (t, J = 8.2 Hz, 1), 6.83 (d, J = 9.2 Hz, 1H), 6.77 (dd, J = 2.4, 8.2 Hz, 1H), 6.67 (s, 2H), 6.66 (t, J = 2.4 Hz, 1H), 6.59 (dd, J = 2.4, 8.2 Hz, 1H), 3.76 (s, 3H); FTIR(KBr) cm^{-1}: 3455, 3351, 1630; EI-MS m/z: 260 $[M]^+$; HR-MS: Calcd for $C_{13}H_{12}N_2O_4$ $[M]^+$: 260.0797. Found 260.0793.

4.1.9. Synthesis of 2-(4-methoxyphenoxy)-4-nitro aniline (4d)

Compound **4d** was obtained in a similar manner to the synthesis of **4a** from **3d**. The product was obtained without purification (279.0 mg, quant.) as a yellow solid: mp: 89–91 °C; ^1H NMR (600 MHz, DMSO-d_6) δ ppm: 7.81 (dd, J = 2.6, 9.2 Hz, 1H), 7.30 (d, J = 2.6 Hz, 1H), 7.07 (d, J = 9.2 Hz, 2H), 7.00 (d, J = 9.2 Hz, 2H), 6.80 (d, J = 8.8 Hz, 1H), 6.70 (s, 2H), 3.77 (s, 3H); FTIR(KBr) cm^{-1}: 3467, 3365, 1627; EI-MS m/z: 260 $[M]^+$; HR-MS: Calcd for $C_{13}H_{12}N_2O_4$ $[M]^+$: 260.0797. Found 260.0802.

4.1.10. Synthesis of *N*-(4-nitro-2-phenoxyphenyl) methanesulfonamide (1a)

A solution of **4a** (500 mg, 2.2 mmol) in anhydrous CH_2Cl_2 (2.2 mL) was treated with dry Et_3N (484 μL, 3.5 mmol) and the mixture was allowed to stir for 1 min at room temperature. To the reaction mixture, CH_3SO_2Cl (840 μL, 10.9 mmol) was added drop-wise at ice-cold temperature. The resulting mixture was stirred for 23 h and the reaction was quenched with distilled water. After extraction with $CHCl_3$, the combined organic phases were dried and filtered, and the solvent was removed in vacuo. To the residue 3 M NaOHaq (10 mL) was added and the mixture stirred at 80–90 °C for 16 h. Afterwards, 5 M HCl was added and it was extracted with $CHCl_3$. The combined organic phases were dried and filtered, and the solvent was removed in vacuo. The residue was purified by chromatography on silica gel with $CHCl_3$/hexane/acetone = 1:8:1 to provide **1a** (497.4 mg, 74.3%) as a pale yellow solid: mp: 142–144 °C (lit[16] mp: 143–144.5 °C); ^1H NMR (600 MHz, DMSO-d_6) δ ppm: 10.16 (s, 1H), 8.03 (dd, J = 2.7, 9.0 Hz, 1H), 7.74 (d, J = 8.8 Hz, 1H), 7.54 (d, J = 2.6 Hz, 2H), 7.49 (t, J = 8.1 Hz, 2H), 7.28 (t, J = 7.0 Hz, 1H), 7.17 (d, J = 8.2 Hz, 2H), 3.20 (s, 3H); FTIR(KBr) cm^{-1}: 3285, 1589, 1521; EI-MS m/z: 308 $[M]^+$; HR-MS: Calcd for $C_{13}H_{12}N_2O_5S$ $[M]^+$: 308.0467. Found 308.0468.

4.1.11. Synthesis of *N*-(2-(2-methoxyphenoxy)-4-nitrophenyl) methanesulfonamide (1b)

Compound **1b** was obtained in a similar manner to the synthesis of **1a** from **4b**. The crude product was purified by chromatography on silica gel with $CHCl_3$/hexane/acetone = 1:8:1 to provide **1b** (91.9 mg, 70.7%) as a yellow solid: mp: 133–134 °C; ^1H NMR (600 MHz, DMSO-d_6) δ ppm: 10.07 (s, 1H), 7.95 (dd, J = 2.6, 8.8 Hz, 1H), 7.69 (d, J = 8.8 Hz, 1H), 7.34 (dt, J = 1.7, 7.9 Hz, 1H), 7.27 (dd, J = 1.5, 8.1 Hz, 1H), 7.24 (dd, J = 1.6, 7.9 Hz, 1H), 7.21 (d, J = 2.6 Hz, 1H), 7.08 (dt, J = 1.5, 7.7 Hz, 1H), 3.75 (s, 3H), 3.23 (s, 3H); FTIR(KBr) cm^{-1}: 3342, 3269, 1602; EI-MS m/z: 338 $[M]^+$; HR-MS: Calcd for $C_{14}H_{14}N_2O_6S$ $[M]^+$: 338.0573. Found 338.0578.

4.1.12. Synthesis of *N*-(2-(3-methoxyphenoxy)-4-nitrophenyl) methanesulfonamide (1c)

Compound **1c** was obtained in a similar manner to the synthesis of **1a** from **4c**. The crude product was purified by chromatography on silica gel with $CHCl_3$/hexane/acetone = 1:8:1 to provide **1c** (88.2 mg, 67.8%) as a pale yellow solid: mp: 121–123 °C; ^1H NMR (600 MHz, DMSO-d_6) δ ppm: 10.14 (s, 1H), 8.03 (dd, J = 2.6, 8.8 Hz, 1H), 7.73 (d, J = 9.2 Hz, 1H), 7.57 (d, J = 2.6 Hz, 1H), 7.38 (t, J = 7.6 Hz, 1H), 6.86 (dd, J = 2.2, 8.2 Hz, 1H), 6.76 (t, J = 2.2 Hz, 1H), 6.71 (dd, J = 2.0, 7.9 Hz, 1H), 3.78 (s, 3H), 3.20 (s, 3H); FTIR (KBr) cm^{-1}: 3244, 1600, 1526; EI-MS m/z: 338 $[M]^+$; HR-MS: Calcd for $C_{14}H_{14}N_2O_6S$ $[M]^+$: 338.0573. Found 338.0575.

4.1.13. Synthesis of *N*-(2-(4-methoxyphenoxy)-4-nitrophenyl) methanesulfonamide (1d)

Compound **1d** was obtained in a similar manner to the synthesis of **1a** from **4d**. The crude product was purified by chromatography on silica gel with $CHCl_3$/hexane/acetone = 1:8:1 to provide **1d** (216.6 mg, 66.6%) as a pale yellow solid: mp: 128–129 °C; ^1H NMR (600 MHz, DMSO-d_6) δ ppm: 10.11 (s, 1H), 7.98 (dd, J = 2.6, 8.8 Hz, 1H), 7.70 (d, J = 8.8 Hz, 1H), 7.41 (d, J = 2.6 Hz, 1H), 7.16 (d, J = 9.2 Hz, 2H), 7.05 (d, J = 9.2 Hz, 2H), 3.79 (s, 3H), 3.22 (s, 3H); FTIR(KBr) cm^{-1}: 3290, 1596, 1522; EI-MS m/z: 338 $[M]^+$; HR-MS: Calcd for $C_{14}H_{14}N_2O_6S$ $[M]^+$: 338.0573. Found 338.0575.

4.2. Evaluation of lipophilicity

The lipophilicity of compounds was evaluated according to the OECD guideline for testing of chemicals 117.[37] The HPLC system is constructed with CCPD pump and UV-8011 (TOSOH Corp., Tokyo, Japan). HPLC analysis was performed using a reversed phase column (COSMOSIL MS-II 4.6 ID × 10 mm guard-column and COSMOSIL MS-II 4.6 ID × 100 mm column, nacalai tesque, Kyoto, Japan) and methanol: phosphate buffer (1/15 mol/L, pH = 7.4) = 70:30 as mobile phase at a flow rate of 1 mL/min, operated at 210 nm (0.005 AUFS). Thiourea, acetanilide, acetophenone, anisole, benzophenone, biphenyl, and dibenzyl were used as reference compounds and unretained organic compound. The calibration graph was based on $Y = 2.07 + 2.13X$ ($X = \log K$, $Y = \log P_{7.4}$, $r^2 = 0.98$). K is capacity factor, derived by the expression: $K = (Rt - t_0)/t_0$ where, Rt (min) is the retention time of the test compound and t_0 (min) is the dead-time measured by unretained organic compound. The retention time of compounds (**1a–d**) was measured by the same method and their $\log P_{7.4}$ values were calculated as shown in Table 1.

4.2.1. In vitro COX-inhibitory potency

Inhibition of COX activity was assayed by using the Colorimetric COX (ovine) Inhibitor Screening Assay kit (Cayman Chemical, No. 760111, Michigan, USA) according to the manufacturer instructions. This assay measures the heme-catalyzed hydroperoxidase activity of ovine COX by monitoring the appearance of oxidized *N*,*N*,*N*′,*N*′-tetramethyl-*p*-phenylenediamine (TMPD). Dimethylsulfoxide (DMSO) (10 μL, control) or a solution of the studied compound in DMSO (10^{-2}–10^{-8} M) was added to a 96-well plate with 0.1 M Tris–HCl assay buffer (pH 8.0) (150 μL), 4.4% solution of heme in DMSO (10 μL) and a solution of ovine COX-1 or COX-2 in 80 mM Tris–HCl (pH 8.0) containing 0.1% Tween 20 and 300 mM diethyldithiocarbamate. After 5 min of pre-incubation at room temperature, a solution of TMPD (20 μL) and arachidonic acid (20 μL) dissolved in 1.1 M ethanol containing 5 mM KOH was added to the mixture. The mixture was incubated for an additional 5 min and the absorbance was read using a plate reader (iMark microplate reader, Bio-Rad Laboratories, Inc., Hercules, CA, USA) at 590 nm. Celecoxib and indomethacin were used as the reference compounds. The IC_{50} values were calculated from the concentration–inhibition response curves. Concentration–inhibition activities (%) were plotted and fitted with sigmoid curves (4 variables), yielding the IC_{50} values. The results are shown in Table 2.

4.2.2. Docking simulations of COX-2

Binding stability was calculated using Discovery Studio 4.0 (Accelrys, Inc., renamed as Dassault Systems Biovia Corp., San Diego, CA, USA). The protein structure of COX-2 was obtained from Protein Data Bank (PDB ID 3QMO). Docking study was performed with CDOCKER program, which calculated protein–ligand interactions (at pH = 8.0), and several docking poses were detected. Scoring the detected poses was performed by calculating intermolecular energy with Generalized Born with Implicit Membrane model.[58] The favorable poses of **1a** and **1d** with the active orientation of the COX-2 pharmacophore at COX-2 active site are shown in Figure 2.

4.3. In vitro transport studies in Caco-2 cells

In vitro transport study was performed according to the literature.[49,50] Caco-2 cell was purchased from ECACC and grown in Eagle's minimal essential medium (Wako Pure Chemical Ind., Ltd, Osaka, Japan) supplemented with 10% fetal bovine serum (Gibco®, Life Technologies, Carlsbad, CA, USA), 1% antibiotic–antimycotic mixed solution (stabilized) and 1% non-essential amino acids (nacalai tesque, Inc., Kyoto, Japan), and incubated at 37 °C in 5% CO_2. Caco-2 cells were seeded at a density of 3.0×10^4 cells/well on porous polyethylene terephthalate membrane filters (3-μm pore size, high density, 0.3 cm^2 filter area, Falcon® cell culture insert, Becton Dickinson, renamed Corning Inc., NY, USA). Cells were cultured in 24-well plates and culture medium was replaced every 2–3 days until using for the assay after seeding 21 days.

TEER of Caco-2 cell monolayers was monitored before assay using Millicell ERS-2 (Merck Millipore, Darmstadt, Germany), and the monolayers with TEER greater than 350 Ω cm^2 were utilized for the assays. For in vitro transport studies, each cell monolayer was washed with phosphate-buffered saline (pH = 7.4) before pre-incubation for 1 h in Hank's balanced salt solution containing Ca, Mg and Phenol Red (HBSS(+)). These assays were initiated by adding the solution of test compounds to the apical (250 μL) or basolateral (950 μL) side at 37 °C. At 1 and 2 h, respectively, after starting the transport experiments, aliquots (50 μL) of medium in the receiver side were collected to determine the transported amount of each compound.

Quantification of test compounds was performed by LC–MS/MS system (TSQ Quantum Discovery, Thermo Fisher Scientific Inc., Waltham, MA, USA). LC condition was as follows: a reverse-phase column (COSMOSIL MS-II 2.0 ID × 150 mm, nacalai tesque, Inc., Kyoto, Japan) was used; the mobile phase was 40% distilled water and 60% acetonitrile containing 0.5% formic acid; and the flow rate was 200 μL/min. Then, the eluent of LC was ionized using the electrospray interface. Full-scan and SRM MS/MS spectra were obtained at negative mode, and parent *m*/*z*, product *m*/*z* and Collision Energy was as follows: **1a** (307.0 *m*/*z*, 229.06 *m*/*z*, 21 V), **1b** (337.1 *m*/*z*, 259.12 *m*/*z*, 21 V), **1c** (337.1 *m*/*z*, 259.13 *m*/*z*, 22 V), and **1d** (337.1 *m*/*z*, 259.10 *m*/*z*, 21 V).

The apparent permeability coefficients (P_{app})(cm/s) were determined according to the following equation:[50]

$$P_{app} = \frac{\Delta Q/\Delta t}{AC_0}$$

where, $\Delta Q/\Delta t$, A, and C_0 represent the linear appearance rate of the compound on the receiver (transported amount/s), the membrane surface area (cm^2), and the initial concentration of compounds in the donor side, respectively. The efflux ratio was calculated using the following equation: efflux ratio = $P_{app,\ B\to A}/P_{app,\ A\to B}$; $P_{app,\ B\to A}$

Table 3
Kinetic parameters for penetration across Caco-2 monolayers

Compounds	1 μM			10 μM		
	$P_{app,\ A\to B}$ (cm/s × 10^{-5})	$P_{app,\ B\to A}$ (cm/s × 10^{-5})	Efflux ratio	$P_{app,\ A\to B}$ (cm/s × 10^{-5})	$P_{app,\ B\to A}$ (cm/s × 10^{-5})	Efflux ratio
Nimesulide (**1a**)	3.78 ± 1.3	2.21 ± 0.4	0.59	3.89 ± 0.3	2.41 ± 0.1*	0.62
o-OCH_3 (**1b**)	1.12 ± 0.3	0.85 ± 0.2	0.76	3.81 ± 1.1	2.54 ± 0.3	0.67
m-OCH_3 (**1c**)	4.27 ± 1.6	4.04 ± 1.8	0.95	5.23 ± 1.1	5.19 ± 1.1	0.99
p-OCH_3 (**1d**)	0.83 ± 0.2	0.68 ± 0.1	0.82	1.82 ± 0.6	0.31 ± 0.2*	0.17

Average ± SD (n = 3).
* Significant decrease compared to $P_{app,\ A\to B}$ ($p < 0.05$).

Table 4
Kinetic parameters for penetration across Caco-2 monolayers with inhibitor (500 μM verapamil)

Compounds	1 μM			10 μM		
	$P_{app,\ A\to B}$ (cm/s × 10^{-5})	$P_{app,\ B\to A}$ (cm/s × 10^{-5})	Efflux ratio	$P_{app,\ A\to B}$ (cm/s × 10^{-5})	$P_{app,\ B\to A}$ (cm/s × 10^{-5})	Efflux ratio
Nimesulide (**1a**)	2.82 ± 0.6	3.95 ± 0.7	1.40	4.71 ± 1.6	6.70 ± 2.0	1.42
p-OCH_3 (**1d**)	3.19 ± 1.2	1.69 ± 0.6	0.53	4.35 ± 0.3	4.18 ± 1.0	0.96

Average ± SD (n = 3).

and $P_{app,\ A\to B}$ represent the P_{app} in the basolateral-to-apical direction and the apical-to-basolateral direction, respectively. The result was shown in Table 3.

The transported amounts of Lucifer yellow (1 mg/mL) and rhodamine123 (5 μM) were also evaluated in parallel. Each quantification was measured on a plate reader (Powerscan® HT, DS Pharma Biomedical Co., Ltd, Osaka, Japan) at 468 nm (λ_{ex}), 530 nm (λ_{em}) for Lucifer yellow and at 485 nm (λ_{ex}), 528 nm (λ_{em}) for rhodamine123. The transported amounts of Lucifer yellow as a *para*-cellular marker was calculated at % transported amount per hour, confirming to be lower than 0.15%/h,[59] whereas that of rhodamine123 was used as a positive control, calculated according to the same procedure as test compounds.[60] To investigate the effects of verapamil, P-gp inhibitor, on efflux of compounds across the Caco-2 cell,[61,62] 500 μM verapamil was loaded into the medium on both sides of the monolayer and pre-incubated for 15 min. The result was shown in Table 4.

Acknowledgements

This research was supported partly by a Grant-in-Aid for Young Scientists from the Japan Society for the Promotion of Science (Nos. 24791331, 26861015). The authors acknowledge Kaori Morimoto Ph.D. lecturer of Tohoku Pharmaceutical University, for valuable discussion on the transport assay. We greatly appreciate Ms. Asuka Okayasu, Ms. Akiyo Oiwa and Ms. Miho Takeda for their technical assistance.

Supplementary data

Supplementary data associated with this article can be found, in the online version, at http://dx.doi.org/10.1016/j.bmc.2015.10.007.

References and notes

1. Ermert, L.; Dierkes, C.; Ermert, M. *Clin. Cancer Res.* **2003**, *9*, 1604.
2. Fournier, D. B.; Gordon, G. B. *J. Cell. Biochem. Suppl.* **2000**, *34*, 97.
3. Howe, L. R.; Subbaramaiah, K.; Brown, A. M.; Dannenberg, A. J. *Endocr. Relat. Cancer* **2001**, *8*, 97.
4. Minghetti, L. *J. Neuropathol. Exp. Neurol.* **2004**, *63*, 901.
5. Hewett, S. J.; Bell, S. C.; Hewett, J. A. *Pharmacol. Ther.* **2006**, *112*, 335.
6. Katori, M.; Majima, M. *Inflamm. Res.* **2000**, *49*, 367.
7. Wu, C.; Li, F.; Niu, G.; Chen, X. *Theranostics* **2013**, *3*, 448.
8. Laube, M.; Kniess, T.; Pietzsch, J. *Molecules* **2013**, *18*, 6311.
9. Channing, M. A.; Simpson, N. *J. Labelled Compd. Radiopharm.* **1993**, *33*, 541.
10. McCarthy, T. J.; Sheriff, A. U.; Graneto, M. J.; Talley, J. J.; Welch, M. J. *J. Nucl. Med.* **2002**, *43*, 117.
11. Toyokuni, T.; Kumar, J. S.; Walsh, J. C.; Shapiro, A.; Talley, J. J.; Phelps, M. E.; Herschman, H. R.; Barrio, J. R.; Satyamurthy, N. *Bioorg. Med. Chem. Lett.* **2005**, *15*, 4699.
12. Tanaka, M.; Fujisaki, Y.; Kawamura, K.; Ishiwata, K.; Qinggeletu; Yamamoto, F.; Mukai, T.; Maeda, M. *Biol. Pharm. Bull.* **2006**, *29*, 2087.
13. Prabhakaran, J.; Underwood, M. D.; Parsey, R. V.; Arango, V.; Majo, V. J.; Simpson, N. R.; Van Heertum, R.; Mann, J. J.; Kumar, J. S. D. *Bioorg. Med. Chem.* **2007**, *15*, 1802.
14. Pacelli, A.; Greenman, J.; Cawthorne, C.; Smith, G. *J. Labelled Compd. Radiopharm.* **2014**, *57*, 317.
15. De Vries, E. F. J.; Doorduin, J.; Dierckx, R. A.; van Waarde, A. *Nucl. Med. Biol.* **2008**, *35*, 35.
16. Takashima-Hirano, M.; Shukuri, M.; Takashima, T.; Goto, M.; Wada, Y.; Watanabe, Y.; Onoe, H.; Doi, H.; Suzuki, M. *Chem. Eur. J.* **2010**, *16*, 4250.
17. Kaur, J.; Tietz, O.; Bhardwaj, A.; Marshall, A.; Way, J.; Wuest, M.; Wuest, F. *ChemMedChem* **2015**, *10*, 1635.
18. Rainsford, K. D. *Inflammopharmacology* **2006**, *14*, 120.
19. Traversa, G.; Bianchi, C.; Da Cas, R.; Menniti-Ippolito, F. M. *BMJ* **2003**, *327*, 18.
20. Li, F.; Chordia, M. D.; Huang, T.; Macdonald, L. *Chem. Res. Toxicol.* **2009**, *22*, 72.
21. Bernareggi, A. *Clin. Pharmacokinet.* **1998**, *35*, 247.
22. Taniguchi, Y.; Yokoyama, K.; Inui, K.; Deguchi, Y.; Furukawa, K.; Noda, K. *Eur. J. Pharmacol.* **1997**, *330*, 221.
23. Toutain, P. L.; Cester, C. C.; Haak, T.; Metge, S. *J. Vet. Pharmacol. Ther.* **2001**, *24*, 35.
24. Suleyman, H.; Cadirci, E.; Albayrak, A.; Halici, Z. *Curr. Med. Chem.* **2008**, *15*, 278.
25. Zrieki, A.; Farinotti, R.; Buyse, M. *Pharm. Res.* **2008**, *25*, 1991.
26. Julemont, F.; de Leval, X.; Michaux, C.; Renard, J. F.; Winum, J. Y.; Montero, J. L.; Damas, J.; Dogne, J. M.; Pirotte, B. *J. Med. Chem.* **2004**, *47*, 6749.
27. Fabiola, G. F.; Pattabhi, V.; Nagarajan, K. *Bioorg. Med. Chem.* **1998**, *6*, 2337.
28. Yamamoto, Y.; Toyohara, J.; Ishiwata, K.; Sano, K.; Yamamoto, F.; Mukai, T.; Maeda, M. *Chem. Pharm. Bull.* **2011**, *59*, 938.
29. Khan, M. N.; Lee, Y. S. *Med. Res. Rev.* **2011**, *31*, 161.
30. Moore, G. G. I.; Harrington, J. K. U.S. Patent 3,840,597, 1974.
31. Sim, Y. L.; Ariffin, A.; Khan, M. N. *J. Org. Chem.* **2007**, *72*, 2392.
32. Chan, D. M. T.; Monaco, K. L.; Wang, R. P.; Winters, M. P. *Tetrahedron Lett.* **1998**, *39*, 2933.
33. Lam, P. Y. S.; Vincent, G.; Clark, C. G.; Deudon, S.; Jadhav, P. K. *Tetrahedron Lett.* **2001**, *42*, 3415.
34. Pike, V. W. *Trends Pharmacol. Sci.* **2009**, *30*, 431.
35. Singh, S.; Sharda, N.; Mahajan, L. *Int. J. Pharm.* **1996**, *176*, 261.
36. Dellis, D.; Giaginis, C.; Tsantili-Kakoulidou, A. *J. Pharm. Biomed. Anal.* **2007**, *44*, 57.
37. OECD, Guidelines for Testing of Chemicals 117, **2004**.
38. Mazak, K.; Noszal, B. *Eur. J. Pharm. Sci.* **2014**, *62*, 96.
39. Mazak, K.; Noszal, B. *J. Med. Chem.* **2012**, *55*, 6942.
40. Wu, G.; Robertson, D. H.; Brooks, C. L., 3rd; Vieth, M. *J. Comput. Chem.* **2003**, *24*, 1549.
41. Michaux, C.; Charlier, C.; Julemont, F.; de Leval, X.; Docne, J. M.; Pirotte, B.; Durant, F. *Eur. J. Med. Chem.* **2005**, *40*, 1316.
42. Ermondi, G.; Caron, G.; Lawrence, R.; Longo, D. *J. Comput. Aided Mol. Des.* **2004**, *18*, 683.
43. Garcia-Nieto, R.; Perez, C.; Gago, F. *J. Comput. Aided Mol. Des.* **2000**, *14*, 147.
44. Alam, M. I.; Beq, S.; Samad, A.; Baboota, S.; Kohli, K.; Ali, J.; Ahuja, A.; Akbar, M. *Eur. J. Pharm. Sci.* **2010**, *40*, 385.
45. Bagal, S.; Bungay, P. *Drug Discovery Today Technol.* **2014**, *12*, e79.
46. Agarwal, S.; Arya, V.; Zhang, L. *J. Clin. Pharmacol.* **2012**, *53*, 228.
47. Mensch, J.; Oyarzabal, J.; Mackie, C.; Augustijns, P. *J. Pharm. Sci.* **2009**, *98*, 4429.
48. Tournier, N.; Valette, H.; Peyronneau, M. A.; Saba, W.; Goutal, S.; Kuhnast, B.; Dolle, F.; Scherrmann, J. M.; Cisternino, S.; Bottlaender, M. *J. Nucl. Med.* **2011**, *52*, 415.
49. Adachi, Y.; Suzuki, H.; Sugiyama, Y. *Pharm. Res.* **2001**, *18*, 1660.
50. Hellinger, E.; Veszelka, S.; Toth, A. E.; Walter, F.; Kittel, A.; Bakk, M. L.; Tihanyi, K.; Hada, V.; Nakagawa, S.; Duy, T. D.; Niwa, M.; Deli, M. A.; Vastag, M. *Eur. J. Pharm. Biopharm.* **2012**, *82*, 340.
51. Josserand, V.; Pelerin, H.; de Bruin, B.; Jego, B.; Kuhnast, B.; Hinnen, F.; Duconge, F.; Boisgard, R.; Beuvon, F.; Chassoux, F.; Daumas-Duport, C.; Ezan, E.; Dolle, F.; Mabondzo, A.; Tavitian, B. *J. Pharmacol. Exp. Ther.* **2006**, *316*, 79.
52. Wang, T.; Sun, Y.; Ma, W.; Yang, Z.; Liu, J.; Fan, H.; Yang, Y.; Gu, J.; Fawcett, J. P.; Guo, Y. *Mol. Pharm.* **2015**, *12*, 1.
53. Seithel, A.; Karlsson, J.; Hilgendorf, C.; Biorquist, A.; Ungell, A. L. *Eur. J. Pharm. Sci.* **2006**, *28*, 291.
54. Giacomini, K. M.; Huang, S. M.; Tweedie, D. J.; Benet, L. Z.; Brouwer, K. L.; Chu, X.; Dahlin, A.; Evers, R.; Fischer, V.; Hilligren, K. M.; Hoffmaster, K. A.; Ishikawa, T.; Keppler, D.; Kim, R. B.; Lee, C. A.; Niemi, M.; Polli, J. W.; Sugiyama, Y.; Swaan, P. W.; Ware, J. A.; Wright, S. H.; Yee, S. W.; Zamek-Gliszczynski, M. J.; Zhang, L. *Nat. Rev. Drug Disc.* **2010**, *9*, 215.
55. Bart, J.; Groen, H. J.; Hendrikse, N. H.; van der Graaf, W. T.; Vaalburg, W.; de Vries, E. G. *Cancer Treat. Rev.* **2000**, *26*, 449.
56. Honjo, H.; Uwai, Y.; Nabekura, T. *Drug Metabol. Drug Interact.* **2014**, *29*, 203.
57. Mabondzo, A.; Bottlaender, M.; Guyot, A. C.; Tsaouin, K.; Deverre, J. R.; Balimane, P. V. *Mol. Pharm.* **2010**, *7*, 1805.
58. Feig, M.; Brooks, C. L., 3rd *Curr. Opin. Struct. Biol.* **2004**, *14*, 217.
59. Hidalgo, I. J.; Raub, T. J.; Borchardt, R. T. *Gastroenterology* **1989**, *96*, 736.
60. Zhu, H. J.; Wang, J. S.; Markowitz, J. S.; Donovan, J. L.; Gibson, B. B.; DeVane, C. L. *Neuropsychopharmacology* **2007**, *32*, 757.
61. Yang, Y.; Bai, L.; Li, X.; Xiong, J.; Xu, P.; Guo, C.; Xue, M. *Toxicol. In Vitro* **2014**, *28*, 388.
62. Tomita, M.; Watanabe, A.; Fujinaga, I.; Yamakawa, T.; Hayashi, M. *Int. J. Pharm.* **2010**, *387*, 1.